INSERTING COMPONENTS INTO GEOMETRIES CONSTRUCTED ONTO A NON-STANDARD SUBSTRATE FOR ELECTRONICS PACKAGING

R.Plant*, S.Chang+, R.Hague*, C.Tuck*, R.Wildman*

*Centre for Additive Manufacturing, The University of Nottingham, Nottingham, NG7 2GX
+Texas Instruments, Inc, 12500 T L Boulevard, Dallas, TX 75243

Abstract

Additive manufacturing (AM) has matured from its initial concept as a prototyping technique to an industrial manufacturing process. Consequently, AM processes must meet relevant standards for an increasing number of applications. Here, we investigate inserting components into geometries constructed onto a silicon nitride substrate, using stereolithography (SLA), for the purpose of electronics packaging. Compared to conventional processes, SLA avoids high temperatures and stresses while permitting much greater flexibility to arrange components in three dimensions. This facilitates an increased feature density and the construction of packages for use in complex spaces. A characteristic of interest to this application, is the SLA material-substrate interaction and the resulting quality of adhesion. The adhesion mechanism between SLA and silicon nitride is investigated and substantially enhanced by a pre-treatment process. A process for then inserting large and complex geometries and components into the SLA build process is identified and compliance of the product with relevant standards is reviewed.

Introduction

The aim of the investigation is to use vat polymerisation, commonly known as stereolithography (SLA), to construct packaging for IC components onto a silicon nitride substrate. The traditional method of encapsulating electronics requires the injection of resin at high temperature and pressure which imposes stress on the component and introduces a failure mechanism. For complex constructions, SLA can provide a cost-effective, alternative to injection moulding [1] with the benefit of comparatively low energy consumption [2] while operating at near ambient temperatures and pressures.

Developing a robust process to package components in three-dimensions or encapsulate them in-situ, can enable an increased feature density to optimise the use of expensive and long lead time substrate materials, and allow the construction of packages for complex spaces. Additionally, functional packaging to complement the operation of the device, and rapid production for bespoke applications can be made possible. It is envisaged that the flexibility of SLA, will yield new solutions and opportunities in this field. However, to achieve these aims, understanding the use of SLA for construction directly onto silicon nitride is required. Specific concerns regard the strength of the bond between the substrate and the product, and the ability to insert multiple large or complex geometries, into the SLA build process.

Prior work

To identify an effective process to promote the adhesion of SLA products on to silicon nitride, the active adhesion mechanisms and methods to enhance them, will be considered. Abbott [3] identifies five primary adhesive mechanisms: intermingling; structural; dissipation; surface energy and chemical bonding. Due to the inability for polymer chains to extend beyond the interface by penetrating the surface of silicon nitride, the mechanism of intermingling is considered infeasible in this application. Other mechanisms can be promoted by different means. For instance, Barhoumi et al [4] increased the surface free energy (SFE) of silicon nitride by approximately 75 percent using chemical treatments. Abbott [3] describes how the energy dissipation mechanism can be promoted by the addition of core shell rubber to mitigate crack propagation. Whereas Zips et al [5] enhanced the chemical bonding between SLA products and silicon containing substrates, including PDMS and glass, through the application of a reactive monolayer.

Ackstaller [6], Tiedje [7] and Grothe [8] measured the adhesive strength of SLA test pieces onto substrates of aluminium oxide, copper, and textiles respectively, without commenting on the mechanism of adhesion. Pasquale [9] produces a finite element model using the cohesion zone model to describe the adhesion between SLA polymers and PMMA (Poly-methyl-methacrylate) in a peel test. Several authors have investigated the adhesion of SLA constructions to silicon wafers [10]–[15]. However, the construction of geometries using SLA specifically onto silicon nitride, has not been identified in the literature. Aspar et al [10] constructed geometries using SLA onto silicon dioxide (SiO2), Silicon mononitride (SiN) and Silicon oxynitride (SiON), with substantial differences in the adhesive shear strength reported despite the materials being chemically similar. The adhesive shear strength between an SLA polymer to SiO_2 was multiplied by nearly nine times [10] by patterning the surface using a diamond saw and introducing structural interlocking. However, the 50-100µm deep channels cut into the surface of the samples tested by Aspar [10] would compromise the thin (200nm - Table 2) Si_3N_4 coating used in the current study. Consequently, this and other mechanically destructive methods are undesirable for this application.

Malengier et al [16] reviewed test methods (shear, peel and tensile) for testing the adhesion of FDM (Fused Deposition Modelling) constructions to textile substrates and concluded the tensile test to be the preferred method. Kendall [17] derives an expression for the tensile separation force required between rigid and elastic materials, bonded by the mechanism of surface energy. In doing so, the following influencing parameters are identified: contact area; surface energy; elastic modulus and Poisson's ratio. To allow comparison with Kendall's equation (Equation 1), a tensile test will be used in this investigation to ascertain the significance of SFE in the adhesion between SLA and silicon nitride. In parallel, core shell rubber will be added to SLA resin to identify if the dissipation mechanism is active and can be enhanced.

The elastic modulus of SLA constructions is known to increase with cross-linking and progressive curing [18]. Consequently, the extent to which post build curing (PBC) and the corresponding change in elastic modulus, can influence adhesion in SLA are of particular interest. The required bond strength of electronics packages onto their substrate, when undergoing a shear test, is quantified in test 2019.9 of the standard MIL-STD-883 [19]. Compliance with the requirements of the standard will be tested during this investigation.

There have been a number of investigations reporting the use of SLA to construct substrates and housings for electronic systems with surface mounted components [6], [20]–[24]. Many of these schemes involve hybrid systems which combine SLA and another AM process. Lopes [25] and MacDonald [26] developed particularly advanced proprietary hybrid AM systems for encapsulating and interconnecting electronic components in three dimensions. However, as explained by Persad [27], hybrid systems possess added complexity, cost and time when switching between processes. Consequently, this investigation is focused on the use of conventional SLA processes.

An SLA construction progresses on a layer-by-layer basis, each with a typical thickness of 25µm to 100µm, depending on the required resolution in the vertical z-axis. Components greater in height than a single layer thickness are termed 'large'. If attempting to insert such a component without intervention, it will clash with the machine's structure. This being either the resin tray in a bottom-up process or the wiper blade in a top-down machine. Tiedje [28] encapsulated a micro light-emitting diode (LED), with a height less than one construction layer, by securing the component to a substrate of a commercially available SLA machine (Formlabs Form 1+). Additionally, as described by Kataria [29], the geometry of a part, for instance one possessing a decreasing cross-sectional area (CSA), may not be possible to insert or will result in cavities. These inserts are termed complex. A solution was identified [29] for inserting complex geometries possessing an inconsistent CSA along a single axis, by using an adaptor piece. These accommodate complex components and convert them to parallel-walled inserts. The application of adaptor pieces can be developed further, with 2-part adaptors to accommodate inserts with a decreasing CSA in multiple axes (Figure 3). Liao et al [30] defined the requirement for adaptor pieces mathematically ('the criterion value'), as a function of the cosine of the angle between; the vector normal to the insert STL surface mesh, and the direction of insertion.

In this paper, relevant properties influencing adhesion of a commercially available SLA material to a silicon nitride substrate are characterised. The adhesion mechanism between the SLA construction and the substrate is investigated and an effective method to promote the adhesive strength, to an extent compliant with the industry standard MIL-STD-883 [19], is reported. Additionally, by building on the work of Tiedje [28] and Kataria [29], a proof of concept for arranging and electrically connecting complex geometries in 3-dimensions within a conventional SLA construction process, is demonstrated.

Methodology

A suite of experiments detailed in Table 1, was identified to examine the strength of adhesion, the underlying mechanism and determine an effective method to promote the adhesion of an SLA polymer onto a silicon nitride substrate. The preferred method was then tested for compliance with MIL-STD-883 test 2019.9 [19] which requires a shear force of 49N to be withstood for the dimensions of the test pieces used. Finally, a method to insert and electrically connect components within an SLA construction was developed. The three potentially active mechanisms identified are now be reviewed in turn.

Surface free energy: The parameters identified in Kendall's model (Equation 1) of SFE adhesion were measured and the influence of PBC characterised (Table 1). The tensile force required to

separate SLA test pieces constructed directly onto silicon nitride, and after progressive PBC, was measured for comparison with Kendall's model. This allows the significance of SFE to be determined and the extent to which PBC influences the adhesive strength established.

Dissipation: To explore the influence of the dissipation mechanism on the adhesion between an SLA polymer and a rigid substrate, core shell rubber was added to Formlabs' clear (FLC) resin in proportions of 5%, 7.5%, 15% and 25% by volume. By adding CSR, it is intended to increase the materials ability to dissipate energy and in turn the required separation force. Shear test pieces, as described by Szeto [31] were constructed using the CSR dosed resin, exposed to progressive PBC and the separation force measured.

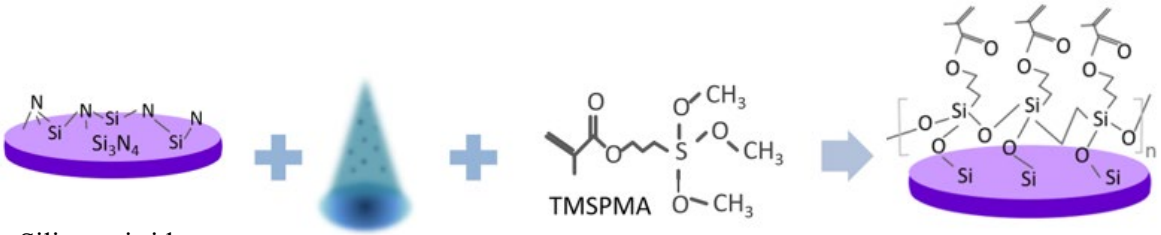

Figure 1: Pre-treatment process for silicon nitride with oxy-plasma and TMSPMA coating to promote adhesion.

Chemical bonding: This was investigated using tensile SLA test pieces constructed directly onto silicon nitride. The substrate was pre-treated (Figure 1) with oxy-plasma to generate hydroxyl groups on the substrate's surface and a monolayer of 3-(Trimethoxysilyl) propyl methacrylate (TMSPMA) applied (Table 1). The silicon in the monolayer forms a covalent bond with the substrate via the hydroxyl groups and the methacrylate tail of the TMSPMA has the capacity to crosslink with the acrylate SLA resin (Equation 1). Constructions onto treated and untreated substrates were then tested for comparison.

Test or activity	Equipment	Methodology
SLA constructions	Formlabs Form 2 SLA machine, Formlabs clear SLA resin.	All SLA products and test pieces were constructed at default settings using 100µm layer thickness. A suitable z-offset was applied when constructing onto substrates, to compensate for their thickness. Test pieces were washed with IPA following construction.
Interfacial energy	Kruss DSA 100 machine	The SFE of SLA polymer slabs was measured using the Owens-Wendt method [32]. The slabs were constructed onto a soda lime glass substrate to improve the surface finish and cured for intervals between 0 and 15 minutes. Surface tension of FLC resin was measured from pendant droplets the Youngs-Laplace method.

Test or activity	Equipment	Methodology
Post build curing	Formlabs Formcure 405nm cure oven	All adhesion test pieces were cured in an inverted position to prevent pooling of any residual liquid resin. When not in use, test pieces were stored in aluminium foil to minimise exposure to ambient light.
Elastic modulus	Solid Microsystems Texture Analyser	Test pieces were mounted in a purposed made stand (Figure 2) to aid consistent exposure during PBC. Tests were performed in accordance with ASTM D638.
Poisson's ratio Tensile strength.	Imetrum gauge optical extensometer	The Poison's ratio of test pieces consistent with D638 was recorded together with the tensile force at break at progressive periods of PBC.
Tensile test	Solid Microsystems Texture Analyser	Tests were performed using a purpose designed bracket and cylindrical test pieces (Figure 2) possessing a contact diameter of 0.85mm and a vertical travel speed of 0.2mm/s. The test pieces were constructed directly onto a silicon nitride substrate.
Shear test (CSR)	Solid Microsystems Texture Analyser. Polycarbonate sheet[+]	Tests were performed using a purpose designed bracket and a tool piece supplied by Mecmesin. The test pieces were designed as described by Szeto [31] with a contact diameter of 11.4mm and constructed directly onto a polycarbonate substrate. A vertical travel speed of 0.1mm/s was used.
Shear test (Mil-STD-883 test 2019.9) [19]	Solid Microsystems Texture Analyser Silicon nitride[$]	The same equipment was used as for the CSR shear tests. Test pieces were designed with dimensions (WLH) of 2.25mm x 2.25mm x 3mm and constructed directly onto silicon nitride. A vertical travel speed of 0.1mm/s was applied.
Plasma treatment	Diener oxy-plasma chamber	The system power was set to 50W and samples of silicon nitride were exposed for 10 minutes.
TMSPMA coating	200ml glass beaker TMSPMA, dry toluene, acetone.	Following oxy-plasma treatment, the samples were immediately immersed in a solution of 2% vol (TMSPMA) in dry toluene, prepared at 50°C and stirred for 1 hr. Upon removal from the solution, the samples were washed in acetone and dried at 50°C in a vacuum oven for 24 hrs.
Surface roughness	Ametek Zygo 8300 coherence scanning interferometer	Silicon nitride samples are tested as received to provide the RMS surface roughness.
Work of adhesion (WoA)	Kruss DSA 100	Calculated using the Young-Dupre method [33] from the pendant drop shape of liquid SLA resin and its sessile droplet contact angle on silicon nitride.

Table 1: Test parameters and equipment

[+]Lexan™ 9030 Polycarbonate sheet [$]Silicon nitride wafer supplied by Inseto™
[*]Paraloid™ BTA-751 core shell rubber supplied by Dow Chemicals™.

Figure 2: Post build cure stand for D638 test pieces.

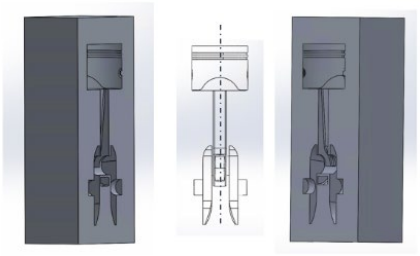

Figure 3: Example piston geometry and 2-part adaptor

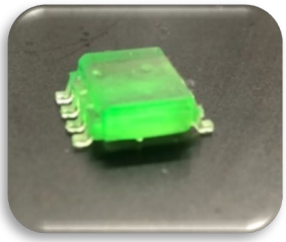

Figure 4: Example semiconductor

Inserting geometries: To demonstrate the insertion of large and complex components, example geometries of a piston (Figure 3) and a semi-conductor package (Figure 4) were downloaded from GrabCAD [34] and constructed using a Anycubic SLA machine. Both the inserts fit the criteria for complex geometries with criterion values [30] <0, necessitating two-part adaptor pieces (Figure 3). The adaptor and corresponding housing were designed using CAD, with clearances of 300-500µm. The adaptor pieces and housing were constructed on a Form 1+ SLA machine, with which a Python interaction can be established via a USB connection. The build process was pre-programmed to pause at the required layers, activate a peel process and raise the platform to the required height as described in Figure 5.

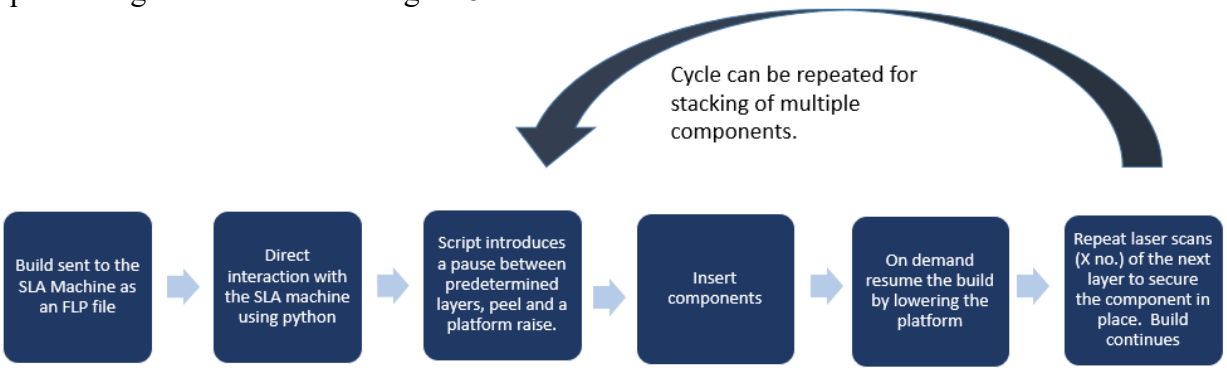

Figure 5: Construction insertion process

Upon pausing at the required layer, the adaptor piece was manually coated with liquid resin and inserted into the housing. This forms a continuous joint between the insert and the package during PBC and secures the insert while inverted until the subsequent layer has been applied to encapsulate the insert. The build was then resumed on demand. During a second planned pause, the adaptor piece containing the semi-conductor package was inserted following the same process.

Interconnectors: An insert (Figure 16) was designed using CAD and constructed with two planned pauses, to allow an LED to be implanted into a purpose designed cavity and the imbedding of a strain gauge. Once these components were in place, wiring was manually routed through purpose designed vias and attached to solderless connectors (Figure 18). A CAD generated housing was then constructed, and the process (Figure 5) repeated with planned pauses at the required layers to receive the insert into the housing and a photo resistor into a designed cavity. Lastly, the housing was sealed to form a 3D electronics package.

Results

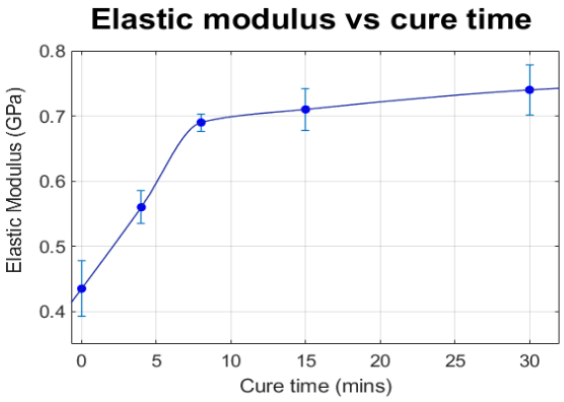

Figure 7: Change in elastic modulus of solidified resin with cure time

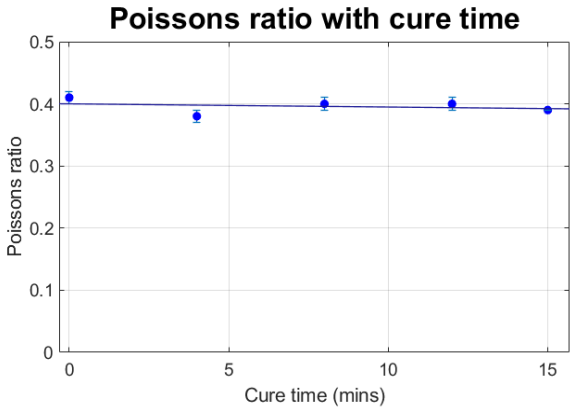

Figure 6: Poisson ratio with cure time

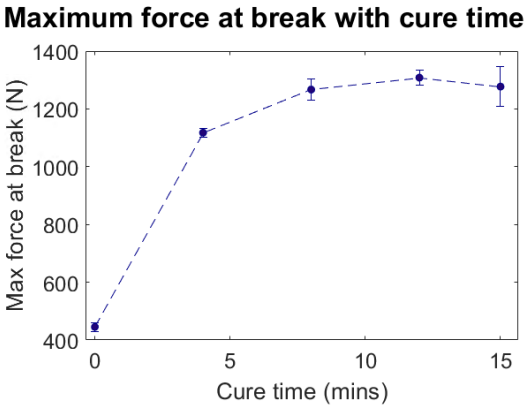

Figure 9: Maximum break force with cure time

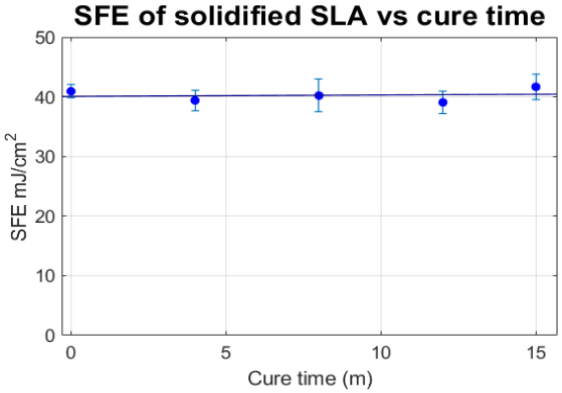

Figure 8: Surface free energy with post build cure time.

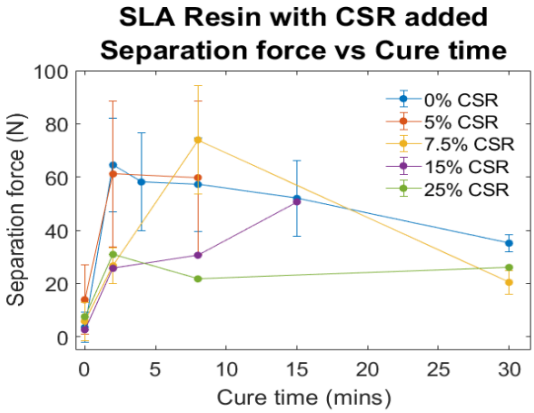

Figure 11: Separation force of SLA resin with CSR added in shear tests (Szeto button) against cure time.

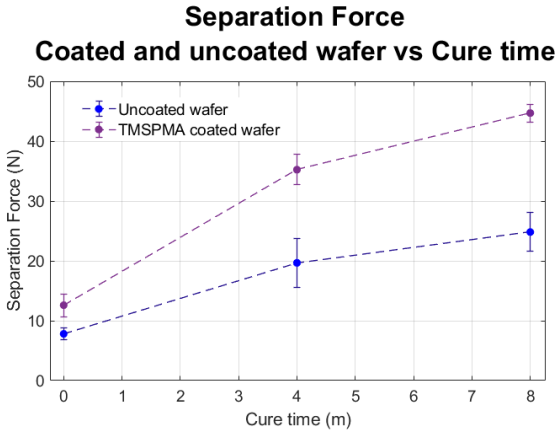

Figure 10: Treated and untreated pull test results on silicon nitride

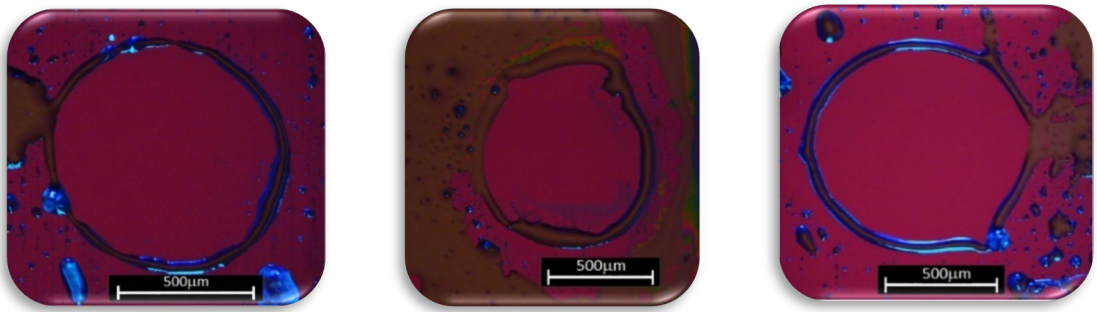

Figure 13: Residual footprints from pull test pieces on untreated silicon nitride without PBC (left), 2 minutes of curing (centre) and 8 minutes of post build curing (right).

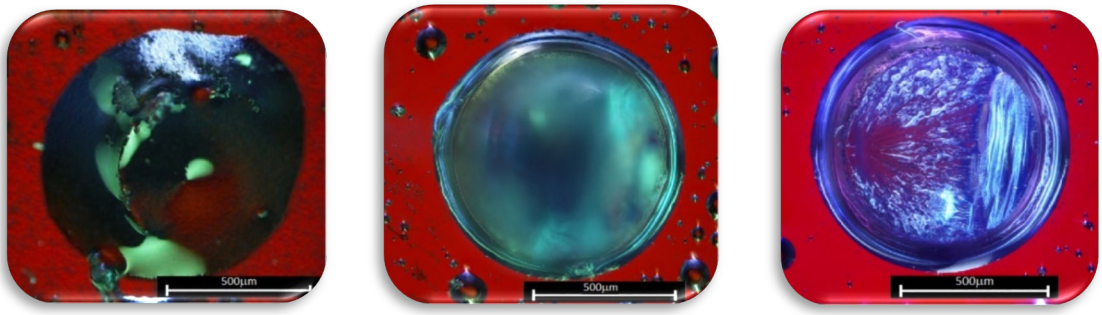

Figure 12: Residue demonstrating cohesion failure of pull test pieces on treated silicon nitride without PBC (left), 2 minutes of PBC (centre) and 8 minutes of PBC (right).

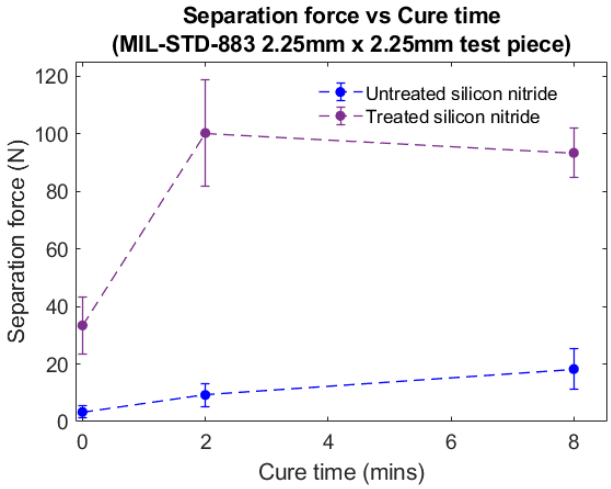

Figure 14: Separation force on treated and untreated shear test pieces

Property	Value
Surface tension of liquid FLC resin (mJ/m^2) (Table 1)	42.77
SFE of silicon nitride (mJ/m^2)	58.13
RMS roughness of silicon nitride substrate (µm)	0.001
Silicon nitride coating thickness (nm) [35]	200
Elastic modulus of silicon nitride (GPa) [36]	160

Table 2: Material properties of SLA resin and silicon nitride substrate samples.

Discussion

Adhesion: The current work investigates the influence of PBC and methods to enhance relevant adhesive mechanisms. The strength of adhesion has been measured to increase with PBC (Figure 11) but not sufficiently on an untreated substrate (Figure 14), to meet the requirements of MIL-STD-883 test 2019.9 [19].

Due to the relatively high elastic modulus and measured surface roughness of silicon nitride (Table 2), the material is considered rigid and perfectly smooth. The SFE of solidified FLC polymer was unchanged during PBC (Figure 9) and comparable to the surface tension of the liquid resin (Table 2). This shows the interfacial energy of the FLC resin to remain substantially unchanged during solidification. The WoA, being a function of interfacial energy, is therefore also assumed to remain constant and applied to Kendall's model (Equation 1) for calculation with the solidified resin. By applying the measured parameters (SFE, elastic modulus, Poisson's ratio and WoA) to Equation 1, an increase in the predictive adhesive strength, from 0.3N to 0.4N after 8 minutes of PBC, can be attributed to the change in properties during PBC.

$$F^2 = \frac{\pi W E d^3}{(1-\nu^2)}$$

Equation 1: The Kendall model describing the detaching force due to work of adhesion.

Where: E is Young's modulus d is the diameter of the disc F is detaching force
ν is Poisson's ratio W_a is Work of adhesion

The SLA test piece will shrink during crosslinking and PBC. Depending on the bond with the substrate and whether slippage [3] occurs, shrinkage will result in either a decrease in the contact area or generate stress at the interface. Internal stress is described by Abbott [37] as "the energy of all adhesion". Any residual stress will contribute to the applied force to initiate and propagate cracking [37]. Therefore, shrinkage and any corresponding reduction in the contact area will only serve to reduce the adhesive strength. Kendall's model (Equation 1) does not consider residual stress from shrinkage and provides a maximum value for adhesion from SFE. This is greatly exceeded by the measured strength of adhesion on untreated substrates (Equation 1) which identifies a more dominant mechanism is active. To satisfy the adhesive requirements of MIL-STD-883 using surface energy, the SFE of the substrate would need to be increased to an unrealistic extent, vastly greater than achieved in the literature [4]. Consequently, methods to increase adhesion through SFE are not explored further.

Figure 15: Stacked piston and semi-conductor geometries.

CSR is used to enhance the bond strength of commercial adhesives by promoting energy dissipation [37]. However, the addition of CSR to the SLA resin did not significantly increase its adhesive strength to silicon nitride (Figure 10). Paraloid™ CSR material was selected for its acrylate shell and anticipated affinity with the FLC acrylate resin. However, it is possible the CSR did not sufficiently bond with the bulk material. If so,

crack energy generated under testing, would continue to propagate through the unbonded CSR/SLA polymer interface, as opposed to being dissipated by the rubber core [37]. Consequently, the mechanism of dissipation cannot be completely discounted as an effective means to promote adhesion.

In contrast to promoting SFE and dissipation, by applying the treatment process described in Figure 1, the chemical bond mechanism between the SLA polymer and the silicon nitride substrate was substantially enhanced and promoted above the cohesive strength of the polymer. This is demonstrated by the failures on the treated substrate being in the stem of the test pieces (Figure 13) instead of at the interface (Figure 12) with untreated substrates. The increase in elastic modulus (Figure 6) due to the progressive cross-linking of polymer chains during PBC, also serves to increase the material's tensile strength (Figure 8). Consequently, the tensile test results on treated substrates (Figure 14), reflect the cohesive strength of the material, and its relationship with PBC. Without PBC, the average adhesive strength (Figure 14) of the treated test pieces was 33.4N compared to 3.3N for untreated silicon nitride. After 2 and 8 minutes of PBC, the average adhesive strength on the treated substrate was increased to 100.2N and 93.3N respectively, with a minimum recorded separation force of 62.3N. Therefore, it is concluded that by applying the described treatment process to a silicon nitride substrate, in conjunction with PBC, the strength of adhesion with the acrylate based FLC resin can be promoted to an extent compliant with, the requirements of MIL-STD-883.

Due to the notably smooth surface (Table 2) of the silicon nitride samples, the adhesive affect of structural interlocking [3] is considered negligible . The experimentation conducted into the respective adhesion mechanisms and their measured influence, indicated that the dominant mechanism between the untreated SLA polymer and silicon nitride, is through chemical bonding. The strength of this bond is observed to increase with exposure to UV light and as the SLA undergoes progressive curing.

Inserting components: The process described (Figure 5) has been demonstrated to be an effective means to insert, large and complex geometries into an SLA build process. This process has been successfully applied to electronic components, which were tested for electrical connectivity and functionality by running a dedicated programme via an Arduino unit connected to a PC. Multiple components can be inserted (Figure 20) and arranged in three dimensions, permitting off-sets and vertical stacking (Figure 15).

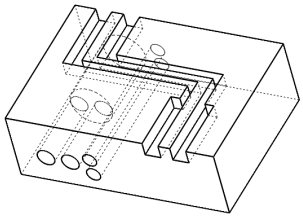

Figure 16: CAD design for insert

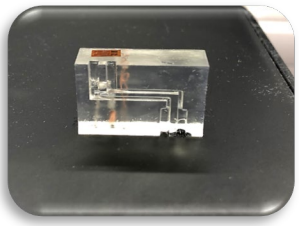

Figure 17: SLA construction of package insert with LED and strain gauge

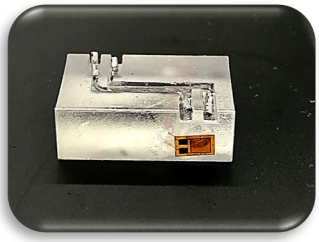

Figure 18: SLA construction of insert with interconnectors

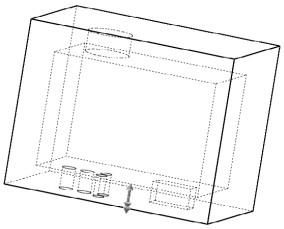

Figure 19: CAD design for housing

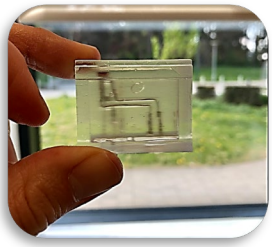

Figure 20: SLA construction of 3D electronics package

Conclusions

This work identifies active adhesion mechanisms between silicon nitride and an SLA polymer. Methods to enhance the mechanisms are investigated and quantified. The physical properties of the silicon nitride samples and the reported experimentation, indicate the dominant adhesion mechanism being via chemical bonding. Through oxy-plasma treatment and the application of a TMPSMA coating, the adhesive strength is substantially enhanced to an extent above the cohesive strength of the SLA material. By pre-treating a silicon nitride substrate with the described process (Table 1), in conjunction with PBC, the adhesive strength of the product has been measured to comply with the requirements defined in the industrial standard MIL-STD-883 [19].

A method for inserting large and complex geometries using adaptor pieces and applying an operation to interrupt and access an in-progress build, has been demonstrated. Additionally, interconnectors have successfully been fitted as a means of connecting components electrically. This demonstrates a concept for constructing 3D electronic modules via a single AM process. Coupled with the method for enhancing adhesion described (Figure 1), this work represents a proof of concept, using SLA, for packaging electronics onto a silicon nitride substrate.

References

[1] N. Hopkinson and P. Dickens, “Analysis of rapid manufacturing - Using layer manufacturing processes for production,” *Proceedings of the Institution of Mechanical Engineers, Part C: Journal of Mechanical Engineering Science*, vol. 217, no. 1, pp. 31–40, 2003, doi: 10.1243/095440603762554596.

[2] Y. Luo, Z. Ji, M. C. Leu, and R. Caudill, “Environmental performance analysis of solid freeform fabrication processes,” *IEEE International Symposium on Electronics and the Environment*, no. February, pp. 1–6, 1999, doi: 10.1109/isee.1999.765837.

[3] S. Abbott, *ADHESION SCIENCE Principles and Practice*. 2015.

[4] H. Barhoumi, A. Maaref, and N. Jaffrezic-Renault, “Experimental study of thermodynamic surface characteristics and pH sensitivity of silicon dioxide and silicon nitride,” *Langmuir*, vol. 26, no. 10, pp. 7165–7173, 2010, doi: 10.1021/la904251m.

[5] S. Zips *et al.*, “Direct Stereolithographic 3D Printing of Microfluidic Structures on Polymer Substrates for Printed Electronics,” *Advanced Materials Technologies*, vol. 4, no. 3, pp. 1–5, 2019, doi: 10.1002/admt.201800455.

[6] L. Lorenz, T. Ackstaller, and K. Bock, “Stereolithographic printed polymers on ceramic for 3D-opto-MID,” p. 12, 2020, doi: 10.1117/12.2554997.

[7] S. Lungen, T. Tiedje, K. Meier, K. Nieweglowski, and K. Bock, “Reliability of 3D additive manufactured packages,” *2018 7th Electronic System-Integration Technology Conference, ESTC 2018 - Proceedings*, 2018, doi: 10.1109/ESTC.2018.8546417.

[8] T. Grothe, B. Brockhagen, and J. L. Storck, “Three-dimensional printing resin on different textile substrates using stereolithography: A proof of concept,” *Journal of Engineered Fibers and Fabrics*, vol. 15, 2020, doi: 10.1177/1558925020933440.

[9] G. de Pasquale, L. Zappulla, L. Scaltrito, and V. Bertana, “Numerical and experimental evaluation of SLA polymers adhesion for innovative bio-MEMS,” *Materials Today: Proceedings*, vol. 7, pp. 572–577, 2019, doi: 10.1016/j.matpr.2018.12.010.

[10] G. Aspar *et al.*, “3D Printing as a New Packaging Approach for MEMS and Electronic Devices,” *Proceedings - Electronic Components and Technology Conference*, no. 1, pp. 1071–1079, 2017, doi: 10.1109/ECTC.2017.119.

[11] L. A. Tse, P. J. Hesketh, D. W. Rosen, and J. L. Gole, “Stereolithography on silicon for microfluidics and microsensor packaging,” *Microsystem Technologies*, vol. 9, no. 5, pp. 319–323, 2003, doi: 10.1007/s00542-002-0254-y.

[12] Y. Kanamori, J. Sato, T. Shimano, S. Nakamura, and K. Hane, “Polymer microstructure generated by laser stereo-lithography and its transfer to silicon substrate using reactive ion etching,” *Microsystem Technologies*, vol. 13, no. 8–10, pp. 1411–1416, 2007, doi: 10.1007/s00542-007-0380-7.

[13] C. Sun, N. Fang, D. M. Wu, and X. Zhang, “Projection micro-stereolithography using digital micro-mirror dynamic mask,” *Sensors and Actuators, A: Physical*, vol. 121, no. 1, pp. 113–120, 2005, doi: 10.1016/j.sna.2004.12.011.

[14] B. Goubault *et al.*, “A New Microsystem Packaging Approach Using 3D Printing Encapsulation Process,” *Proceedings - Electronic Components and Technology Conference*, vol. 2018-May, no. Figure 5, pp. 118–124, 2018, doi: 10.1109/ECTC.2018.00026.

[15] P. J. H. A.Choudhury, “Novel method SL alignment of MEMS,” 2003.

[16] B. Malengier, C. Hertleer, L. Cardon, and L. van Langenhove, “3D Printing on Textiles: Testing of Adhesion,” *Journal of Fashion Technology & Textile Engineering*, vol. s4, no. October, 2018, doi: 10.4172/2329-9568.s4-013.

[17] K.Kendall, *Molecular adhesion and its applications; The Sticky Universe*. 2001.

[18] X. Chen, I. A. Ashcroft, C. J. Tuck, Y. F. He, R. J. M. Hague, and R. D. Wildman, “An investigation into the depth and time dependent behavior of UV cured 3D ink jet printed objects,” *Journal of Materials Research*, vol. 32, no. 8, pp. 1407–1420, 2017, doi: 10.1557/jmr.2017.4.

[19] “MIL-STD-883K Department of defense, test method standard for microcircuits.” 2016.

[20] V. Palazzi *et al.*, “3-D-Printing-Based Selective-Ink-Deposition Technique Enabling Complex Antenna and RF Structures for 5G Applications up to 6 GHz,” *IEEE Transactions on Components, Packaging and Manufacturing Technology*, vol. 9, no. 7, pp. 1434–1447, 2019, doi: 10.1109/TCPMT.2019.2919187.

[21] T. Tiedje, S. Lungen, K. Nieweglowski, and K. Bock, “Will 3D-semiadditive packaging with high conductive redistribution layer and process temperatures below 100°C enable new electronic applications?,” *2018 7th Electronic System-Integration Technology Conference, ESTC 2018 - Proceedings*, pp. 6–10, 2018, doi: 10.1109/ESTC.2018.8546450.

[22] G. Fei, T. Wei, Q. Shi, Y. Guo, H. Oprins, and S. Yang, “Preliminary study on hybrid manufacturing of the electronic-mechanical integrated systems (EMIS) via the LCD stereolithography technology,” *Solid Freeform Fabrication 2019: Proceedings of the 30th Annual International Solid Freeform Fabrication Symposium - An Additive Manufacturing Conference, SFF 2019*, pp. 2028–2036, 2019.

[23] J. Li *et al.*, “Hybrid additive manufacturing of 3D electronic systems,” *Journal of Micromechanics and Microengineering*, vol. 26, no. 10, 2016, doi: 10.1088/0960-1317/26/10/105005.

[24] T. Ackstaller, L. Lorenz, K. Nieweglowski, and K. Bock, “Combination of Thick-Film Hybrid Technology and Polymer Additive Manufacturing for High-Performance Mechatronic Integrated Devices,” *Proceedings of the International Spring Seminar on Electronics Technology*, vol. 2019-May, pp. 1–6, 2019, doi: 10.1109/ISSE.2019.8810205.

[25] A. J. Lopes, E. MacDonald, and R. B. Wicker, “Integrating stereolithography and direct print technologies for 3D structural electronics fabrication,” *Rapid Prototyping Journal*, vol. 18, no. 2, pp. 129–143, 2012, doi: 10.1108/13552541211212113.

[26] E. MacDonald *et al.*, “3D printing for the rapid prototyping of structural electronics,” *IEEE Access*, vol. 2, no. December, pp. 234–242, 2014, doi: 10.1109/ACCESS.2014.2311810.

[27] J. Persad and S. Rocke, “A Survey of 3D Printing Technologies as Applied to Printed Electronics,” *IEEE Access*, vol. 10, no. December 2019, pp. 27289–27319, 2022, doi: 10.1109/ACCESS.2022.3157833.

[28] T. Tiedje, S. Lungen, M. Schubert, M. Luniak, K. Nieweglowski, and K. Bock, “Will Low-Cost 3D Additive Manufactured Packaging Replace the Fan-Out Wafer Level Packages?,” *Proceedings - Electronic Components and Technology Conference*, pp. 1065–1070, 2017, doi: 10.1109/ECTC.2017.276.

[29] A. Kataria and D. W. Rosen, “Building around inserts: Methods for fabricating complex devices in stereolithography,” *Rapid Prototyping Journal*, vol. 7, no. 5, pp. 253–261, 2001, doi: 10.1108/13552540110410459.

[30] Y. S. Liao, H. C. Li, and M. T. Chen, “The study of rapid prototyping process with embedded functional inserts,” *Journal of Materials Processing Technology*, vol. 192–193, no. 1, pp. 68–74, 2007, doi: 10.1016/j.jmatprotec.2007.04.042.

[31] W. K. Szeto, M. Y. Xie, J. K. Kim, M. M. F. Yuen, P. Tong, and S. Yi, “Interface failure criterion of button shear test as a means of interface adhesion measurement in plastic packages,” *International Symposium on Electronic Materials and Packaging, EMAP 2000*, pp. 263–268, 2000, doi: 10.1109/EMAP.2000.904165.

[32] D. K. Owens, “Estimation of the surface free energy of polymers,” *Journal of Applied Polymer Science*, vol. 13, pp. 1741–1747, 1969.

[33] U.Okoroanyanwu, *Chemistry and Lithography*. 2010.

[34] “Stratasy Solutions Ltd; Grabcad.” Grabcad.com (accessed Mar. 07, 2022).

[35] Inseto, “Technical data sheet for silicon nitride wafer.” 2021.

[36] A. Khan, J. Philip, and P. Hess, “Young’s modulus of silicon nitride used in scanning force microscope cantilevers,” *Journal of Applied Physics*, vol. 95, no. 4, pp. 1667–1672, 2004, doi: 10.1063/1.1638886.

[37] S. Abbott, *Sticking together: The science of adhesion*. 2020.